The Unusually Stable Quaternary Structure of Human Cu,Zn-Superoxide Dismutase 1 Is Controlled by Both Metal Occupancy and Disulfide Status*[S]

Fabio Arnesano‡, Lucia Banci‡, Ivano Bertini‡§, Manuele Martinelli‡, Yoshiaki Furukawa¶‖, and Thomas V. O'Halloran¶**

From the ‡Magnetic Resonance Center CERM and Department of Chemistry, University of Florence, Via Luigi Sacconi 6, 50019 Sesto Fiorentino, Florence, Italy and ¶Departments of Chemistry and Biochemistry, Molecular Biology, and Cell Biology, Northwestern University, Evanston, Illinois 60208

The eukaryotic copper,zinc superoxide dismutases are remarkably stable dimeric proteins that maintain an intrasubunit disulfide bond in the reducing environment of the cytosol and are active under a variety of stringent denaturing conditions. The structural interplay of conserved disulfide bond and metal-site occupancy in human copper,zinc superoxide dismutase (hSOD1) is of increasing interest as these post-translational modifications are known to dramatically alter the catalytic chemistry, the subcellular localization, and the susceptibility of the protein to aggregation. Using biophysical methods, we find no significant change in the gross secondary or tertiary structure of the demetallated form upon reduction of the disulfide. Interestingly, reduction does lead to a dramatic change in the quaternary structure, decreasing the monomer-to-dimer equilibrium constant by at least four orders of magnitude. This reduced form of hSOD1 is monomeric, even at concentrations well above the physiological range. Either the addition of Zn(II) or the formation of the disulfide leads to a shift in equilibrium that favors the dimeric species, even at low protein concentrations (*i.e.* micromolar range). We conclude that only the most immature form of hSOD1, *i.e.* one without any post-translational modifications, favors the monomeric state under physiological conditions. This finding provides a basis for understanding the selectivity of mitochondrial SOD1 import and may be relevant to the toxic properties of mutant forms of hSOD1 that can cause the familial form of amyotrophic lateral sclerosis.

Eukaryotic copper,zinc superoxide dismutase (SOD1)[1] catalyzes the dismutation of superoxide radical to oxygen and hydrogen peroxide and is a 32-kDa homodimeric enzyme found predominantly in the cytosol (1). SOD1 is one of the most thermally stable enzymes known in mesophilic organisms. Dismutase activity declines at 80 °C with a corresponding melting temperature, T_m, above 90 °C (2). The protein is stable in the presence of strong denaturants, and the activity is observed in 4% SDS or 10 M urea (3). Structural properties of SOD1 that contribute to this extreme thermochemical stability are thought to include an eight-stranded β-barrel motif, hydrophobic interactions associated with dimerization, coordinate covalent bonds, and an intrasubunit disulfide bond between highly conserved pair of cysteines, namely Cys[57] and Cys[146] in the human form. Whereas the dimerization can contribute to the structural stability through the reduction of its mobility (4), the roles of the disulfide bond in the SOD1 function and/or structure are only now beginning to emerge. Inspection of the SOD1 structure reveals that the loop containing Cys[57] can influence the conformation of the catalytically important residue, Arg[143], through a hydrogen-bonding network (5). Portions of this loop contribute to the dimer interface (6), leading to the possibility that the disulfide bond influences the protein dimerization and thereby the SOD1 quaternary structure.

To attain the correctly folded quaternary structure and become enzymatically active, several post-translational modifications need to occur in SOD1 such as the acquisition of copper and zinc ions, formation of the disulfide bond, and dimerization. Whereas the mechanism by which SOD1 acquires Zn(II) is not fully understood, several aspects of the copper insertion by the copper chaperone for SOD1 (CCS) are well established (7–12). More recently, Furukawa *et al.* (13) have shown that the intrasubunit disulfide bond is correctly introduced in yeast SOD1 by the copper-bound form of yeast CCS. However, given that the cytosol is a strongly reducing environment due to the high GSH/GSSG ratio (100:1–1000:1) (14), the disulfide formation is an unfavorable process. Those results suggest that the immature disulfide-reduced hSOD1 is a more important species in the cytosolic environment than previously thought.

§ To whom correspondence may be addressed: CERM and Dept. of Chemistry, University of Florence, Via L. Sacconi 6, Sesto Fiorentino 50019, Italy. Tel.: 39-055-45-4272; Fax: 39-055-4574271; E-mail: bertini@cerm.unifi.it.

** To whom correspondence may be addressed: Dept. of Chemistry, Northwestern University, 2145 Sheridan Rd., Evanston, Illinois 60208. Tel.: 847-491-5060; Fax: 847-491-7713; E-mail: t-ohalloran@northwestern.edu.

[1] The abbreviations used are: SOD1, Cu,Zn-superoxide dismutase; hSOD1, human SOD1; ySOD1, yeast SOD1; E,E-hSOD1^{SH}, fully reduced and demetallated hSOD1; E,Zn-hSOD1^{SH}, fully reduced Zn-loaded hSOD1; E,E-hSOD1^{SS}, oxidized and demetallated hSOD1; E,Zn-hSOD1^{SS}, oxidized and Zn-loaded hSOD1; Q133M2SOD1, human SOD1 with the mutations F50E/G51E/E133Q; CCS, copper chaperone for SOD1; AMS, 4-acetamide-4′-maleimidylstilbene-2,2′-disulfonic acid; WT, wild type; HSQC, heteronuclear single quantum coherence; CD, circular dichroism; fALS, familial form of amyotrophic lateral sclerosis.

Field *et al.* (15) have also recently shown that uptake of the SOD1 molecule into the intermembrane space of the mitochondria is dependent on the status of the disulfide bond. The reduced form of SOD1 is imported through the mitochondrial outer membrane, but the disulfide-bonded apo-SOD1, the Zn(II)-loaded SOD1, and the holo-form or fully mature form of SOD1 are not readily transferred from the cytosol into the intermembrane space of the mitochondria. The effects of disulfide reduction on the SOD1 structure are therefore relevant to our understanding of the intracellular localization and stability of the SOD1 molecule. In this study we show that, even after removal of both copper and zinc ions from the active and mature form of hSOD1, the dimeric state still persists; however, upon reduction of the disulfide bond, the protein can readily dissociate to the monomer form. Zn(II) addition to the reduced apo-hSOD1 restores the dimeric state, indicating that only the most immature form of hSOD1 before any post-translational modifications favors the monomeric state. These results provide a molecular basis for understanding factors that control the SOD1 monomer-dimer equilibrum in the cytosol and have direct relevance to models for the toxic gain of function mutations in SOD1 that are associated with familial amyotrophic lateral sclerosis (fALS).

EXPERIMENTAL PROCEDURES

Sample Preparation—hSOD1 was expressed in the *Escherichia coli* TOPP1 (Stratagene) or BL21(DE3) strain. The mutations were performed using a QuikChange™ site-directed mutagenesis kit (Stratagene). The ^{15}N-labeled protein in which the non-conserved cysteine residues, Cys[6] and Cys[111], were mutated to Ser was obtained by growing the cells in the M9 minimal medium with N^{15}-NH$_4$Cl following a reported procedure (16), whereas LB medium was used for the non-labeled protein. The cells were grown at 37 °C until A_{600} = 0.6 and induced with 1.0 mM isopropyl 1-thio-β-D-galactopyranoside for 6 h. The protein was isolated and purified according to previously published protocols (16). Fully reduced and demetallated hSOD1 (E,E-hSOD1^{SH}) was prepared by treating the isolated protein with dithiothreitol at 37 °C for 1 h in an anaerobic chamber to reduce the disulfide bond (13). The protein solution was then acidified using 0.4% trifluoroacetic acid, and organic solvents (15% CH$_3$CN, 10% CH$_3$OH) were included to remove the metal ions. The protein solution was purified using reverse-phase high pressure liquid chromatography through a 300-Å C18 Jupiter column (Phenomenex) equilibrated with 0.1% trifluoroacetic acid in water. The fractions containing hSOD1 were eluted with a linear gradient of 0.1% trifluoroacetic acid in CH$_3$CN and lyophilized. The metal content of E,E-hSOD1 was checked by inductively coupled plasma atomic emission spectrometry using a Thermo Jarrell Ash Atomscan Model 25 Sequential inductively coupled spectrometer, and zinc and copper ions were <10 nM in the 2 μM protein sample. Zinc reconstitution was obtained as previously described (17). Protein reduction and metallation were carried out under a nitrogen atmosphere in an anaerobic chamber.

Thiol-Disulfide Reduction Assay—The thiol-disulfide status of purified hSOD1 was determined by chemical modification with the thiol-specific reagent 4-acetamide-4′-maleimidylstilbene-2,2′-disulfonic acid (AMS) (Molecular Probes, Inc.) (13). AMS conjugation results in a ~1 kDa increase in the molecular mass of hSOD1 as visualized by non-reducing SDS-PAGE and Coomassie Blue staining. 3 μg of the SOD1 protein that is dissolved in 10 μl of the buffer was mixed with 2.5 μl of 100 mM AMS and 2.5 μl of 10% SDS. The reaction mixture was incubated at 37 °C for an hour in an anaerobic chamber, and then the Laemmli buffer without any reducing agent was added. After boiling at 95 °C for 2 min, the sample was loaded on SDS-PAGE gel.

CD Spectroscopy—Far-UV CD spectra (185–260 nm) of hSOD1 were recorded on JASCO J-810 spectropolarimeter. A cell with a path length of 1 mm was used for the measurement, and the parameters were set as follows: bandwidth, 2 nm; step resolution, 0.1 nm; scan speed, 50 nm/min; and response time: 2 s. Each spectrum was obtained as the average of five scans. The protein concentration was typically around 20 μM. Prior to the calculation of the mean residue molar ellipticity, all of the spectra were corrected by subtracting the contributions from the buffer. Spectra were then smoothed using adjacent averaging or Fast Fourier transform filter. Quantitative estimations of the secondary

structure contents were made using the DICROPROT software package (18).

NMR Spectroscopy—Data were collected on Bruker Avance 500 spectrometer, operating at a proton nominal frequency of 500.13 MHz. A triple resonance Cryoprobe equipped with pulsed field gradients along the *z*-axis was used. The two-dimensional ^{1}H-^{15}N HSQC spectra and relaxation experiments were acquired on 0.5 mM samples of ^{15}N-labeled E,E- and E,Zn-hSOD1^{SH} in 20 mM sodium phosphate buffer (pH 7.0). The ^{15}N backbone longitudinal and transverse relaxation rates, R_1 and R_2, were measured as previously described (19). The value of reorientational correlation time τ_m was estimated from the R_2/R_1 ratio with the program Quadric_diffusion (20). All of the spectra were collected at 298 K, processed using the standard Bruker software (XWINNMR). All of the NMR samples were prepared under nitrogen atmosphere in a glove box where they were loaded into 5-mm quartz NMR tubes capped with latex serum caps.

Gel Filtration Chromatography—200 μl of 30 μM hSOD1 protein was loaded on Superose 12 HR 10/30 (Amersham Biosciences) at 4 °C. The column was preequilibrated with 50 mM potassium phosphate, pH 7.5, and the flow rate was 1.0 ml/min. To prevent the possible air-oxidation of the thiol groups, 1 mM dithiothreitol was added in the above buffer for the gel filtration analysis of E,E- and E,Zn-hSOD1^{SH}. For the experiments using E,E-hSOD1$^{SH/SS}$, 0.1 mM EDTA was included in the buffer. The chromatogram was obtained by monitoring the absorbance at 215 nm. The calibration of the column for the estimation of molecular weight was performed using 200 μl of 0.25 g/liter immunoglobulin G, bovine serum albumin, ovalbumin, carbonic anhydrase, horse heart skeletal myoglobin, *E. coli* thioredoxin, and aprotinin as protein standards.

RESULTS

Chemical reduction of the disulfide in hSOD1 with dithiothreitol followed by acidification to remove bound metal ions yields the fully reduced and demetallated E,E-hSOD1^{SH} sample as confirmed by AMS modification and inductively coupled plasma atomic emission spectrometry analysis. In the NMR and CD studies, two of the four Cys residues in hSOD1 have been mutated to Ser (*i.e.* C6S/C111S) to avoid the possible oxidation of the free thiol groups and it has been reported that these Cys residues, Cys[6] and Cys[111], which are not involved in disulfide formation, have little effects on the SOD1 activity and structure (21). When the disulfide bond is intact, previous studies have shown that SOD1 is mainly comprised of β sheets and has little α-helical structure (19). To examine the possible structural changes upon disulfide reduction, CD spectroscopy was used to probe the secondary structure.

Disulfide Reduction Has a Little Effect on the SOD1 Secondary Structure—As seen in Fig. 1, the CD spectrum of the most immature form, E,E-hSOD1^{SH}, exhibits a negative peak at 207 nm, indicating that E,E-hSOD1^{SH} is predominantly comprised of the β sheets (22). The absence of a strong band at 222 nm in the spectrum indicates low α-helical content (22). We attempted to see whether any major changes in the secondary structure upon the disulfide formation could be detected by using E,E-form of the monomeric hSOD1 mutant, E,E-Q133M2SOD1^{SS}. However, both E,E-hSOD1^{SH} and E,E-Q133M2SOD1^{SS} give CD signals similar to that of the matured form of the enzyme, Cu,Zn-hSOD1^{SS} (Fig. 1). The fitting of CD data (18, 23) suggests that these forms of hSOD1 have similar secondary structure content as reported in Table I. Disulfide reduction does not significantly alter the secondary structure, suggesting that several features of the β barrel-folding pattern are acquired before any post-translational modifications. We also examined the effects of the disulfide reduction on the tertiary and quaternary structure of hSOD1 by NMR spectroscopy.

Disulfide Reduction and Zinc Removal Disrupt SOD1 Quaternary Structure—The two-dimensional ^{1}H-^{15}N HSQC spectrum of E,E-hSOD1^{SH} is shown in Fig. 2A (*red contours*). Although several signals are present in a spectral region typical of unfolded polypeptides (between 8 and 8.5 ppm in the ^{1}H

Thiol-Disulfide Status Alters SOD1 Monomer Formation

FIG. 1. **The CD spectra of E,E-hSOD1^{SH}(C6S/C111S) (*broken curve*), E,E-Q133M2SOD1^{SS} (*solid curve*), and Cu,Zn-hSOD1^{SS}(C6S/C111S) (*dotted curve*) in 20 mM sodium phosphate buffer, pH 7.0.** 20 μM protein was used for the measurements.
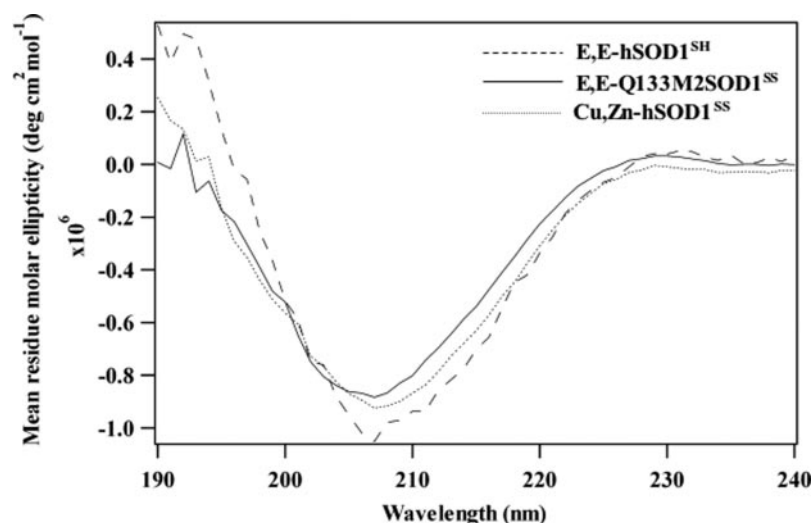
TABLE I

Secondary structure content of various forms of hSOD1 obtained from the fitting of far-UV CD spectra by the DICROPROT software package (18) using the least square method of Chen et al. (23)

	α Helix	β Sheet	Random coil
	%		
E,E-hSOD1^{SH}	8	50	42
E,E-Q133M2SOD1^{SS}	4	46	50
Cu,Zn-hSOD1^{SS}	6	43	51

dimension), this spectrum is remarkably similar to that of E,E-Q133M2SOD1^{SS} (Fig. 2*B*) for which the NMR signals have been assigned (19). This finding suggests that the tertiary structure of E,E-hSOD1^{SH} also is similar to that of E,E-Q133M2SOD1^{SS}, *i.e.* the β barrel structure is maintained, and loops IV (residues 45–85) and VII (residues 121–142) are severely disordered (19). Because loop IV contains three His ligands involved in Zn(II) binding and also involves a disulfide-bond residue, namely Cys^{57}, it is likely that zinc removal and disulfide reduction can destabilize and increase the structural mobility of loop IV. Likewise, it has been reported that loop VII, which produces an optimal electrostatic field for uptake of the superoxide substrate, becomes well organized upon the zinc binding (19, 24). Therefore, even after demetallation and reduction of the disulfide bond, most of the protein tertiary structure is retained with the exception of the disorder of some loop regions.

However, when zinc ion is added to the E,E-hSOD1^{SH} sample, a dramatic change in the ^{1}H-^{15}N HSQC spectrum is observed (Fig. 2*A*, *blue contours*). Compared with the E,E state, E,Zn-hSOD1^{SH} shows a larger signal dispersion in the spectrum, which resembles that of the matured protein, Cu,Zn-hSOD1^{SS} (Fig. 2*C*). Monomeric E,Zn-Q133M2SOD1^{SS} shows the intermediate features in the HSQC spectrum between monomeric E,E-hSOD1^{SH} and dimeric Cu,Zn-hSOD1^{SS} (see Supplemental Fig. S1). The ^{1}H and ^{15}N chemical shift differences between the three zinc-bound forms of the protein are shown in Fig. 3 as the weighted average chemical shift differences, Δ_{avg}(HN) (*i.e.* {[(ΔH)^2 + (ΔN/5)^2]/2}$^{1/2}$, where ΔH and ΔN are chemical shift differences for ^{1}H and ^{15}N, respectively). Differences between E,Zn-hSOD1^{SH} and E,Zn-Q133M2SOD1^{SS} (Fig. 3*A*) are due to disulfide reduction and/or dimerization, differences between E,Zn-hSOD1^{SH} and Cu,Zn-hSOD1^{SS} (Fig. 3*B*) are due to disulfide reduction and/or copper binding, and differences between E,Zn-Q133M2SOD1^{SS} and Cu,Zn-hSOD1^{SS} (Fig. 3*C*) are due to dimerization and/or copper binding. In all of the cases, significant chemical shift differences are present

in loops IV and VII, whereas those for the residues at the N- and C-terminal regions are relatively small. The disulfide formation/copper binding in the zinc-bound proteins affects loops IV and VII more significantly than the N- and C-terminal regions, which are at the dimer interface. Cross-peaks of some of these residues at the dimer interface, which are outside the crowded regions and well resolved in ^{1}H-^{15}N HSQC spectra, are indicated with *arrows* in Fig. 2, *A–D*.

The overall correlation time for molecular reorientation (τ_m) provides insights into the hSOD1 quaternary structure. The τ_m values were estimated from the averaged values of ^{15}N R_1 and R_2, which are obtained for 69 and 72 backbone NH resonances of E,E- and E,Zn-hSOD1^{SH}, respectively (Table II). The overall correlation time is highly sensitive to the protein size (25), and the dimerization is expected to increase τ_m. Estimated from the R_2/R_1 ratios, τ_m is significantly larger in E,Zn-hSOD1^{SH} (20.6 $\pm$ 0.9 ns) than in E,E-hSOD1^{SH} (10.3 $\pm$ 0.4 ns). In particular, the τ_m value of E,E-hSOD1^{SH} is very similar to that of monomeric E,E-Q133M2SOD1^{SS} (10.1 ns) (19) and E,Zn-Q133M2SOD1^{SS} (8.4 $\pm$ 0.3 ns) (24), whereas E,Zn-hSOD1^{SH} exhibits a τ_m value similar to that found for dimeric Cu,Zn-hSOD1^{SS} (25.3 ns) (4). These results suggest that E,E-hSOD1^{SH} is monomeric and that Zn(II) addition to the reduced protein can lead to the dimerization. This result is quite surprising, because previous studies have shown that SOD1 dimer is very stable, even after complete demetallation (26). To directly examine the effects of the disulfide reduction on the monomer-dimer equilibrium at physiological concentrations of protein, we employed gel filtration chromatography.

Monomer-Dimer Equilibrium of E,E- and E,Zn-hSOD1$^{SH/SS}$— Fig. 4*A* compares the gel filtration chromatograms between the wild-type E,E- and E,Zn-hSOD1^{SH} proteins. The E,E-form of reduced hSOD1(WT) favors the monomeric state at the concentration of ~30 μM (*broken curve* in Fig. 4*A*). The physiological concentration of SOD1 in the cell has been estimated to be ~10 μM in yeast by quantitative Western blot (8) and ~100 μM in the cytosol of cultured hepatocytes by quantitative immunocytochemistry (27). After E,E-hSOD1^{SH}(WT) is anaerobically incubated with an equimolar amount of zinc ion for an hour at 37 °C, the resultant protein, E,Zn-hSOD1^{SH}(WT), strongly favors the dimeric state (*solid curve* in Fig. 4*A*). The preference for the monomeric state in E,E-hSOD1^{SH}(WT) can be also confirmed by using a hSOD1 mutant in which all of the Cys residues are changed to Ser, C6S/C57S/C111S/C146S (*i.e.* the C^{4}S form). The protein conformation of reduced hSOD1 can be modeled by this quadruple mutant, which cannot undergo any type of thiol oxidation. Consistent with the WT data, the E,E-form of this C^{4}S
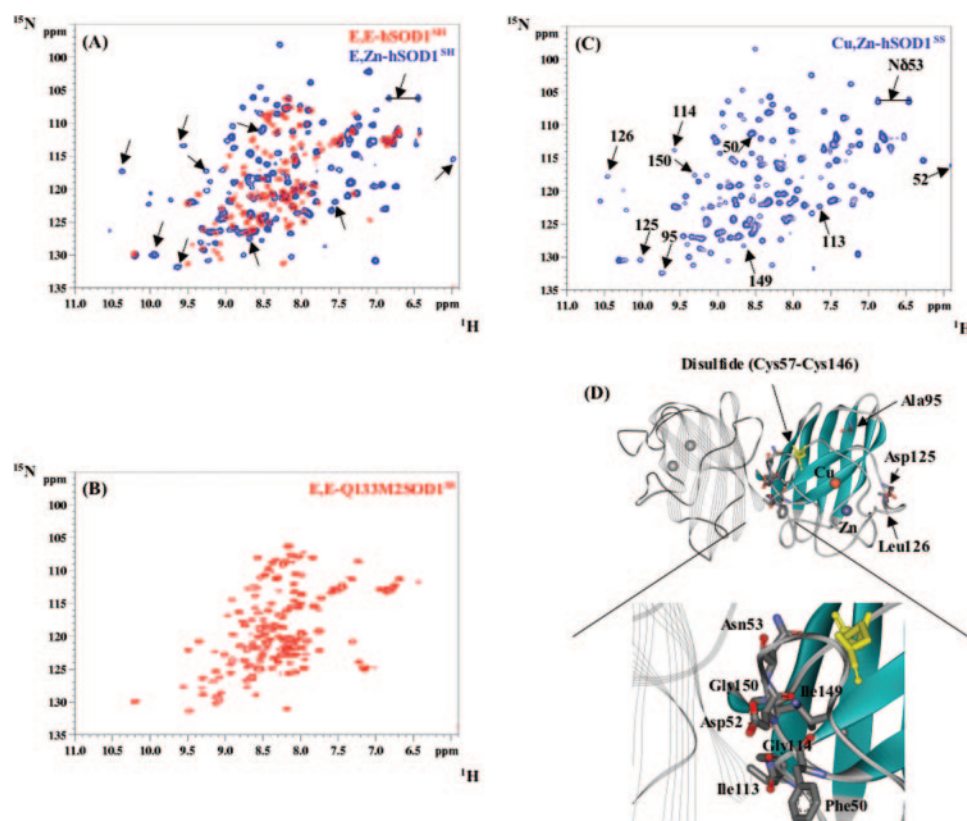
FIG. 2. **The two-dimensional ^{1}H-^{15}N HSQC spectra of E,E-hSOD1^{SH}(C6S/C111S) (*A, red contours*) and E,Zn-hSOD1^{SH}(C6S/C111S) (*blue contours*), monomeric E,E-Q133M2SOD1^{SS} (*B*), and dimeric Cu,Zn-hSOD1^{SS}(C6S/C111S) (*C*).** Some cross-peaks of residues at the dimer interface and in the metal binding region are indicated by *arrows* and are shown in *D*.

mutant favors the monomeric state and turns to the dimeric state upon the addition of the zinc ion (Fig. 4*B*).

To investigate the effects of the conserved disulfide bond (Cys^{57}-Cys^{146}) on monomer-dimer equilibrium, the non-conserved cysteine residues, Cys^6 and Cys^{111}, were mutated to Ser. As seen in the WT protein, the E,E-form of the C6S/C111S mutant favors the monomeric state when the disulfide bond is reduced and the addition of Zn ion can dimerize the protein (Fig. 4*C*). These results show that the monomer-dimer equilibrium is not affected by the non-conserved cysteine residues. In contrast, when the conserved Cys residues are oxidized to form the intramolecular disulfide bond, the E,E-hSOD1^{SS}(C6S/C111S) form elutes at the peak position corresponding to the dimeric state (*broken curve* in Fig. 4*D*). This result suggests that, in the absence of any metal ions, the SOD1 monomerization is promoted by reduction of the canonical disulfide. The addition of Zn(II) ion to E,E-hSOD1^{SS}(C6S/C111S) does not further change the elution profile, and E,Zn-hSOD1^{SS}(C6S/C111S) still favors the dimeric state (*solid curve* in Fig. 4*D*). Therefore, Zn(II) removal alone cannot monomerize the hSOD1 protein unless the disulfide is reduced. We conclude that the nascent or folded form of the hSOD1 polypeptide favors the monomer state until it undergoes the first of several post-translational modifications in the cell.

DISCUSSION

The subunits of copper,zinc superoxide dismutase are not linked by covalent bonds but are nonetheless unusually resistant to dissociation. Strong interaction is observed under extreme denaturing conditions such as 8–10 M urea, 7 M guanidine HCl, or SDS (3). Accordingly, it is surprising that the E,E-hSOD1^{SH} protein is monomeric, even without any detergents present. In fact, we find that the E,E-hSOD1^{SH} form is dominantly monomeric even at the high concentrations (500

μM) used in the NMR experiments. When we assume that ~10% total 500 μM E,E-hSOD1^{SH} is in the dimeric state, the upper limit for the association constant is estimated as $K_a < 2 \times 10^2$ M^{-1}. At the other extreme, E,E-hSOD1^{SS} still favors the dimeric state, even at the low concentrations used (30 μM) in the gel filtration experiments. Based on a conservative estimate of the absorbance in the gel filtration, <10% of the total E,E-hSOD1^{SS} exists as the monomer in this condition, leading to an estimate of the lower limit of $K_a > 3 \times 10^6$ M^{-1}. Thus, although disulfide formation does not significantly change the secondary structure of hSOD1 (Fig. 1), it clearly favors dimerization by at least four orders of magnitude. The observations here show that the disulfide bond plays a quite significant but not clearly exclusive role in determining the quaternary structure of the human form of SOD1.

Zinc acquisition by the E,E-hSOD1^{SH} state seems to have as profound effect on the monomer-dimer equilibrium as disulfide formation, *i.e.* both E,E-hSOD1^{SS} and E,Zn-hSOD1^{SH} favor the dimeric state, even when protein concentration is as low as 10 μM. Zinc binding has been shown to reduce the mobility of the loop IV (residues 48–85, *colored* with *purple* in Fig. 5) (19, 24), which contains the important amino acid residues for zinc ligation, *i.e.* His^{63}, His^{71}, and His^{80} (*colored* with *green* in Fig. 5). Because loop IV in SOD1 is adjacent to the interface between the subunits, such a structurization of loop IV upon the binding of the Zn ion is also implicated to play important roles in the SOD1 dimerization (19, 24). The results here show that, even when the disulfide is reduced, Zn(II) binding alone is enough to stabilize a conformation of the protein that favors dimer formation. Likewise, it is interesting to note that loop IV is linked to the β sheet unit via the disulfide formation between Cys^{57} and Cys^{146}. Whereas a structural determination of several SOD1 microstates is currently in progress, reduction of the

(A) E,Zn-hSOD1^{SH} - E,Zn-hSOD1^{SS}(Q133M2)

(B) E,Zn-hSOD1^{SH} - Cu,Zn-hSOD1^{SS}

(C) E,Zn-hSOD1^{SS}(Q133M2) - Cu,Zn-hSOD1^{SS}
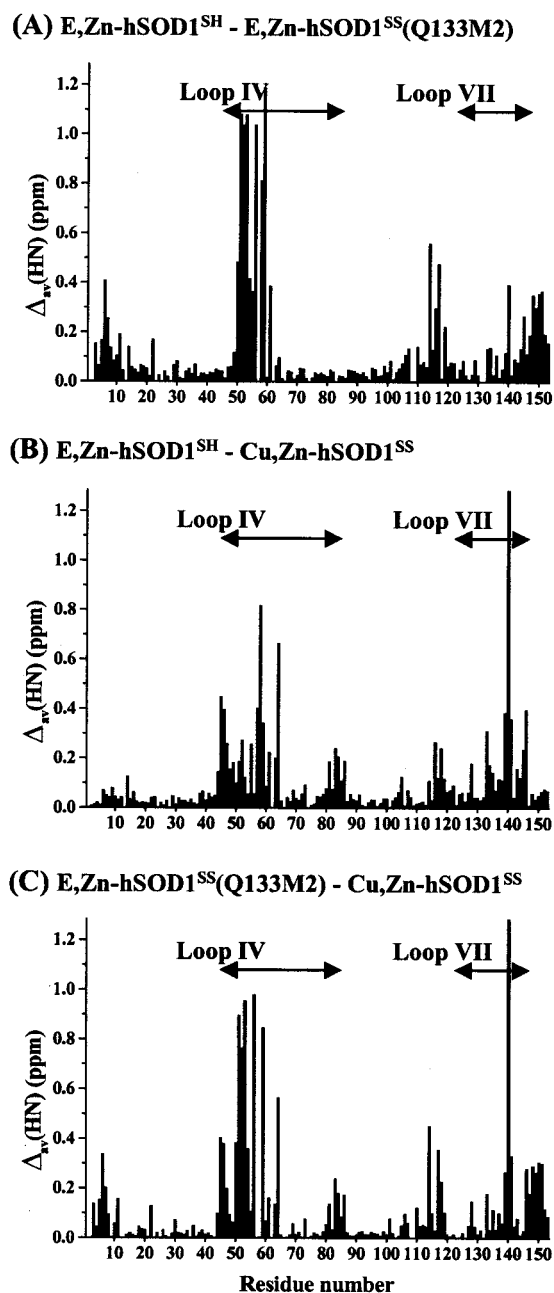

FIG. 3. **^{1}H and ^{15}N amide chemical shift differences between E, Zn-hSOD1^{SH} and E,Zn-Q133M2SOD1^{SS} (*A*), between E,Zn-hSOD1^{SH} and Cu,Zn-hSOD1^{SS} (*B*), and between E,Zn-Q133M2SOD1^{SS} and Cu,Zn-hSOD1^{SS} (*C*).** The weighted average chemical shift differences $\Delta_{avg}(HN)$ are shown (see "Results"). The extents of loops IV and VII are indicated with *arrows*.

TABLE II
Average ^{15}N R_1 and R_2 values and the overall correlation time, τ_m

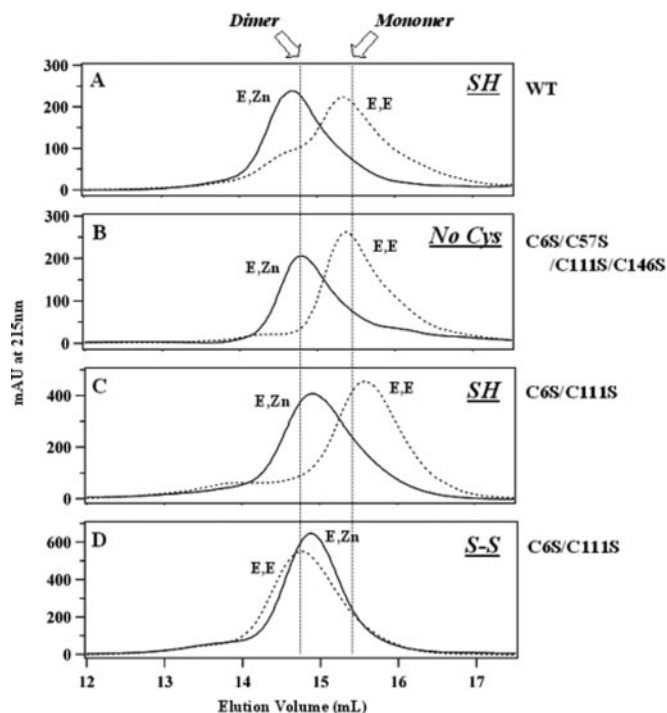|	Average R_1	Average R_2	τ_m
	s^{-1}		ns
E,E-hSOD1^{SH}	1.79 ± 0.17^a	13.8 ± 2.0^a	10.3 ± 0.4
E,Zn-hSOD1^{SH}	1.01 ± 0.10^a	29.2 ± 3.4^a	20.6 ± 0.9
E,E-Q133M2SOD1^{SS}	1.24 ± 0.09^b	12.6 ± 2.7^b	10.1 ± 0.3^c
E,Zn-Q133M2SOD1^{SS}	1.36 ± 0.29^b	13.4 ± 0.9^b	8.4 ± 0.3^d
Cu,Zn-hSOD1^{SS}	0.60 ± 0.11^b	33.9 ± 4.1^b	25.3 ± 1.3^e

[a] Measured at 500 MHz.
[b] Measured at 600 MHz.
[c] Ref. 19.
[d] Ref. 24.
[e] Ref. 4.

FIG. 4. **The chromatograms of the gel filtration experiments using hSOD1^{SH}(WT) (*A*), hSOD1(C6S/C57S/C111S/C146S) (*B*), hSOD1^{SH}(C6S/C111S) (*C*), and hSOD1^{SS}(C6S/C111S) (*D*).** The *solid* and *broken curves* represent E,Zn- and E,E-forms of each protein, respectively. The elution profiles were obtained by using Superose 12 (Amersham Biosciences) column and monitoring the absorbance change at 215 nm. The flow rate was 1 ml/min.
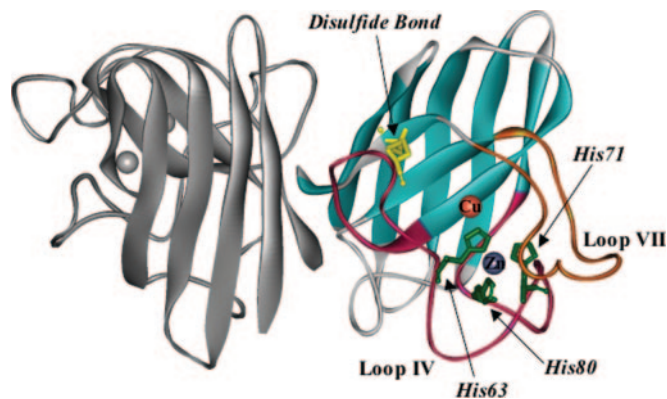

FIG. 5. **The structure of E,Zn-hSOD1^{SS} (Protein Data Bank code 1HL4).** The disulfide bond and the zinc ligands are shown as *yellow* and *green sticks*, respectively. Copper and zinc ions are indicated in the sphere style. Loop IV (residues 48–85) is colored *purple*, whereas loop VII (residue 121–142) is colored *orange*.

disulfide bond would release and disorder loop IV, resulting in the increase of its conformational flexibility. Such a disordered structure of loop IV may obstruct the interaction between the subunits. Therefore, both disulfide formation and Zn(II) binding can add structure to the protein conformation around loop IV, which would promote the interaction between the subunits.

Important roles of the disulfide bond in the monomer-dimer equilibrium have also been reported in the yeast SOD1 (ySOD1) and are in accordance with this study on human SOD1. However, Furukawa *et al.* (13) have found that reduction of the disulfide in E,Zn-ySOD1^{SS} (dimer) leads to conformation changes that favor the monomeric state under the same conditions. Thus, there is an interesting difference in the behavior of the yeast and human proteins. The E,Zn-form of reduced human protein favors the dimeric state, whereas the

same state of the yeast protein favors the monomer state. Although the structural characterization of E,Zn-ySOD1^{SH} and E,Zn-hSOD1^{SH} is necessary, we speculate that this difference may be attributed to two proline residues, Pro^{142} and Pro^{144}, near the intrasubunit disulfide bond that are present in the yeast but not in the human protein. Culotta and co-workers (28) have recently shown that these residues play a key role in the CCS-independent activation pathways, which differ for the yeast and human enzyme. The trans-configuration of these proline residues would limit the ySOD1 conformation, especially around the disulfide bond and loop IV to reduce the interaction between the subunits. Given that the cytosol can provide the strongly reducing conditions (100–1000:1 of the GSH/GSSG ratio), the monomeric form of this disulfide-reduced SOD1 protein appears to be more physiologically relevant than has been appreciated to date.

In the yeast system, the most immature form, *i.e.* E,E-ySOD1^{SH}, is the only one that is efficiently taken up from the cytosol into the intermembrane space of mitochondria. Mitochondrial retention of SOD1 is dependent upon its activation by yeast CCS inside the intermembrane space of mitochondria (15); however, once the Zn(II) ion is incorporated or the disulfide bond is introduced in E,E-ySOD1^{SH}, mitochondrial import of the SOD1 protein is significantly inhibited (15). This selectivity for SOD1 mitochondrial import could be explained by our current results. The completely demetallated and disulfide-reduced form has a smaller size than any other forms. Furthermore, it is expected to be easier to unfold and thread its way through machinery in the mitochondrial outer membrane. Dimerization that accompanies metallation and disulfide formation may prevent the SOD1 dimer from crossing the mitochondrial membrane.

Perturbation of the SOD1 quaternary structure by disulfide reduction may be relevant to the etiology of fALS, which has been associated with a number of mitochondrial pathologies in fALS patients (29). Point mutations in the human SOD1 can cause 20% of total fALS, which is a fatal and late-onset neurodegenerative disorder (30, 31). The fALS-associated mutants do not necessarily lose the SOD1 activity but gain some new activities to cause the disease, such as peroxidase activity or adventitious protein aggregation (29). It has been suggested that the apoform of the fALS mutant exhibits decreased stability, which has some correlations with disease duration (32). Furthermore, it has been proposed that protein monomerization plays a role in formation of misfolded intermediates, leading to protein aggregation (33). Because the conserved disulfide bond in SOD1 is adjacent to the dimer interface (Fig. 4) (34), we suspect that SOD1 monomerization can increase the exposure of these Cys residues. A thiol group in the Cys residue is in general susceptible to the oxidative modification, which plays an important role in the protein aggregation in some neurodegenerative disease (35). Recently, it has been shown that exposed Cys residues in the SOD1 monomer can be modified by oxidative stress, leading to disulfide-linked multimerization of SOD1 (13). These SOD1 multimers could be involved in protein aggregation and the pathology of amyotrophic lateral sclerosis. Interestingly, increased susceptibility to disulfide reduction has been observed in some fALS mutants (36); therefore, protein monomerization caused by the disulfide reduction and demetallation might be an important process in causing the fALS diseases.

REFERENCES

1. McCord, J. M., and Fridovich, I. (1969) *J. Biol. Chem.* **244,** 6049–6055
2. Roe, J. A., Butler, A., Scholler, D. M., Valentine, J. S., Marky, L., and Breslauer, K. J. (1988) *Biochemistry* **27,** 950–958
3. Forman, H. J., and Fridovich, I. (1973) *J. Biol. Chem.* **248,** 2645–2649
4. Banci, L., Bertini, I., Cramaro, F., Del Conte, R., Rosato, A., and Viezzoli, M. S. (2000) *Biochemistry* **39,** 9108–9118
5. Fisher, C. L., Cabelli, D. E., Tainer, J. A., Hallewell, R. A., and Getzoff, E. D. (1994) *Proteins* **19,** 24–34
6. Bertini, I., Mangani, S., and Viezzoli, M. S. (1998) in *Advanced Inorganic Chemistry* (Sykes, A. G., ed) pp. 127–250, Academic Press, San Diego
7. O'Halloran, T. V., and Culotta, V. C. (2000) *J. Biol. Chem.* **275,** 25057–25060
8. Rae, T. D., Schmidt, P. J., Pufahl, R. A., Culotta, V. C., and O'Halloran, T. V. (1999) *Science* **284,** 805–808
9. Rae, T. D., Torres, A. S., Pufahl, R. A., and O'Halloran, T. V. (2001) *J. Biol. Chem.* **276,** 5166–5176
10. Lamb, A. L., Torres, A. S., O'Halloran, T. V., and Rosenzweig, A. C. (2000) *Biochemistry* **39,** 14720–14727
11. Culotta, V. C., Klomp, L. W. J., Strain, J., Casareno, R. L. B., Krems, B., and Gitlin, J. D. (1997) *J. Biol. Chem.* **272,** 23469–23472
12. Eisses, J. F., Stasser, J. P., Ralle, M., Kaplan, J. H., and Blackburn, N. J. (2000) *Biochemistry* **39,** 7337–7342
13. Furukawa, Y., Torres, A. S., and O'Halloran, T. V. (2004) *EMBO J.* **23,** 2872–2881
14. Hwang, C., Sinskey, A. J., and Lodish, H. F. (1992) *Science* **257,** 1496–1502
15. Field, L. S., Furukawa, Y., O'Halloran, T. V., and Culotta, V. C. (2003) *J. Biol. Chem.* **278,** 28052–28059
16. Banci, L., Benedetto, M., Bertini, I., Del Conte, R., Piccioli, M., and Viezzoli, M. S. (1998) *Biochemistry* **37,** 11780–11791
17. Beem, K. M., Rich, W. E., and Rajagopalan, K. V. (1974) *J. Biol. Chem.* **249,** 7298–7305
18. Deleage, G., and Geourjon, C. (1993) *Comput. Appl. Biosci.* **9,** 197–199
19. Banci, L., Bertini, I., Cramaro, F., Del Conte, R., and Viezzoli, M. S. (2003) *Biochemistry* **42,** 9543–9553
20. Bruschweiler, R., Liao, X., and Wright, P. E. (1995) *Science* **268,** 886–889
21. Parge, H. E., Hallewell, R. A., and Tainer, J. A. (1992) *Proc. Natl. Acad. Sci. U. S. A.* **89,** 6109–6113
22. Greenfield, N., and Fasman, G. D. (1969) *Biochemistry* **8,** 4108–4116
23. Chen, Y. H., Yang, J. T., and Chau, K. H. (1974) *Biochemistry* **13,** 3350–3359
24. Banci, L., Bertini, I., Cantini, F., D'Onofrio, M., and Viezzoli, M. S. (2002) *Protein Sci.* **11,** 2479–2492
25. Einstein, A. (1956) *Investigations on the Theory of the Brownian Movement*, Dover, New York
26. Hartz, J. W., and Deutsch, H. F. (1972) *J. Biol. Chem.* **247,** 7043–7050
27. Chang, L. Y., Slot, J. W., Geuze, H. J., and Crapo, J. D. (1988) *J. Cell Biol.* **107,** 2169–2179
28. Carroll, M. C., Girouard, J. B., Ulloa, J. L., Subramaniam, J. R., Wong, P. C., Valentine, J. S., and Culotta, V. C. (2004) *Proc. Natl. Acad. Sci. U. S. A.* **101,** 5964–5969
29. Julien, J. P. (2001) *Cell* **104,** 581–591
30. Deng, H. X., Hentati, A., Tainer, J. A., Iqbal, Z., Cayabyab, A., Hung, W. Y., Getzoff, E. D., Hu, P., Herzfeldt, B., Roos, R. P., *et al.* (1993) *Science* **261,** 1047–1051
31. Gurney, M. E., Pu, H., Chiu, A. Y., Dal Canto, M. C., Polchow, C. Y., Alexander, D. D., Caliendo, J., Hentati, A., Kwon, Y. W., Deng, H. X., Chen, W., Zhai, P., Sufit, R. L., and Siddique, T. (1994) *Science* **264,** 1772–1775
32. Lindberg, M. J., Tibell, L., and Oliveberg, M. (2002) *Proc. Natl. Acad. Sci. U. S. A.* **99,** 16607–16612
33. Rakhit, R., Crow, J. P., Lepock, J. R., Kondejewski, L. H., Cashman, N. R., and Chakrabartty, A. (2004) *J. Biol. Chem.* **279,** 15499–15504
34. Bordo, D., Djinovic, K., and Bolognesi, M. (1994) *J. Mol. Biol.* **238,** 366–386
35. Lee, S., and Eisenberg, D. (2003) *Nat. Struct. Biol.* **10,** 725–730
36. Tiwari, A., and Hayward, L. J. (2003) *J. Biol. Chem.* **278,** 5984–5992

Access the most updated version of this article at doi: 10.1074/jbc.M406021200

Alerts:
- When this article is cited
- When a correction for this article is posted

Click here to choose from all of JBC's e-mail alerts

Supplemental material:
http://www.jbc.org/content/suppl/2004/09/09/M406021200.DC1

This article cites 34 references, 20 of which can be accessed free at
http://www.jbc.org/content/279/46/47998.full.html#ref-list-1